Article

Current Biology

Accelerating effects of growing-season warming on tree seasonal activities are progressively disappearing

Highlights

- Acceleration of tree seasonal activities due to growing-season warming slows down
- Positive effect of growing-season warming on productivity is declining
- Warming responses of tree phenology and productivity are linearly correlated
- Temperature sensitivities of phenology and productivity are linked to water stress

Authors

Yuxin Qiao, Hongshuang Gu, Hanfeng Xu, ..., Nicholas G. Smith, Jianquan Liu, Lei Chen

Correspondence

lei.chen1029@gmail.com

In brief

Temporal changes in the effects of growing-season warming on trees' spring and autumn phenology are not yet clear. Qiao et al. find that growing-season warming leads to earlier tree phenological events in spring and autumn, but the accelerating effects on phenology are disappearing in the deciduous broadleaved forests in the Northern Hemisphere.

Qiao et al., 2023, Current Biology *33*, 1–9
September 11, 2023 © 2023 Elsevier Inc.
https://doi.org/10.1016/j.cub.2023.07.030

CellPress

Please cite this article in press as: Qiao et al., Accelerating effects of growing-season warming on tree seasonal activities are progressively disappearing, Current Biology (2023), https://doi.org/10.1016/j.cub.2023.07.030

Current Biology

CellPress

Article

Accelerating effects of growing-season warming on tree seasonal activities are progressively disappearing

Yuxin Qiao,[1,5] Hongshuang Gu,[1,5] Hanfeng Xu,[1] Qimei Ma,[1] Xin Zhang,[1] Qin Yan,[1] Jie Gao,[2] Yuchuan Yang,[1] Sergio Rossi,[3] Nicholas G. Smith,[4] Jianquan Liu,[1] and Lei Chen[1,6,*]

[1]Key Laboratory of Bio-Resource and Eco-Environment of Ministry of Education, College of Life Sciences, Sichuan University, Chengdu 610064, China

[2]College of Life Sciences, Xinjiang Normal University, Urumqi 830054, China

[3]Département des Sciences Fondamentales, Université du Québec à Chicoutimi, Chicoutimi, QC G7H 2B1, Canada

[4]Department of Biological Sciences, Texas Tech University, Lubbock, TX 79409, USA

[5]These authors contributed equally

[6]Lead contact

*Correspondence: lei.chen1029@gmail.com

https://doi.org/10.1016/j.cub.2023.07.030

SUMMARY

The phenological changes induced by climate warming have profound effects on water, energy, and carbon cycling in forest ecosystems. In addition to pre-season warming, growing-season warming may drive tree phenology by altering photosynthetic carbon uptake. It has been reported that the effect of pre-season warming on tree phenology is decreasing. However, temporal change in the effect of growing-season warming on tree phenology is not yet clear. Combining long-term ground observations and remote-sensing data, here we show that spring and autumn phenology were advanced by growing-season warming, while the accelerating effects of growing-season warming on tree phenology were progressively disappearing, manifesting as phenological events converted from being advanced to being delayed, in the temperate deciduous broadleaved forests across the Northern Hemisphere between 1983 and 2014. We further observed that the effect of growing-season warming on photosynthetic productivity showed a synchronized decline over the same period. The responses of phenology and photosynthetic productivity had a strong linear relationship with each other, and both showed significant negative correlations with the elevated temperature and vapor pressure deficit during the growing season. These findings indicate that warming-induced water stress may drive the observed decline in the responses of tree phenology to growing-season warming by decelerating photosynthetic productivity. Our results not only demonstrate a close link between photosynthetic carbon uptake and tree seasonal activities but also provide a physiological perspective of the nonlinear phenological responses to climate warming.

INTRODUCTION

Tree phenology, periodical biological events in trees, influences the fitness and distribution of trees as well as water, energy, and carbon cycling of forest ecosystems.[1,2] Under climate warming, shifts in tree phenology, such as advanced spring leaf-out and delayed autumn leaf senescence, have been widely observed.[3,4] However, the physiological mechanisms underlying the shifts in tree phenology in response to warming remain unclear, which hinders a reliable prediction of future tree phenology.

Numerous studies have reported that climate warming can influence spring phenology by altering the accumulations of chilling and forcing units, which are necessary to break endodormancy and ecodormancy before the onset of bud burst.[5,6] It is noted that trees need to assimilate and store sufficient carbohydrates in the preceding growing season to support growth reactivation in the following spring.[7,8] Accordingly, spring phenology is also likely to depend on the photosynthetic carbon assimilation during the previous growing season. Gu et al. recently demonstrated that spring leaf-out occurred earlier with the increase in temperature and photosynthetic carbon assimilation during the previous growing season in temperate and boreal forests,[9] while experimental evidence showed that decreased carbohydrates storage by shading significantly delayed spring budbreak in shade-intolerant species but advanced it in shade-tolerant species.[10] Despite conflicting findings, it is reported that photosynthetic carbon assimilation is also linked to autumn phenology. For example, Zani et al. found that a warmer growing season led to earlier leaf senescence by accelerating carbon assimilation in temperate trees.[11] Lu and Keenan, however, failed to detect a significant negative relationship between growing-season carbon uptake and autumn senescence.[12] Therefore, it remains unclear whether and how growing-season warming affects spring and autumn phenological events in trees.

Please cite this article in press as: Qiao et al., Accelerating effects of growing-season warming on tree seasonal activities are progressively disappearing, Current Biology (2023), https://doi.org/10.1016/j.cub.2023.07.030

Generally, temperature during the pre-season, which is characterized as a period when the mean temperature is associated with the timing of tree phenology prior to the start of phenological events,[13,14] is often considered as the most influential factor controlling tree phenology. Recent studies have observed that the advanced effect of pre-season warming on spring phenology is declining, even delaying spring phenology,[15,16] possibly as a result of warming-induced changes in chilling[15] or forcing accumulations,[17] but none have particularly examined the temporal variations in the effect of growing-season warming on spring or autumn phenology. Under heat-induced water stress, trees tend to close stomas to diminish water loss through transpiration in leaves, but this also blocks CO_2 uptake.[18] Therefore, leaf photosynthetic rate is expected to decrease when growing-season temperatures (T_{GS}) exceed the thermal optimum.[19,20] This heat-induced decrease in photosynthesis might constrain the accelerated impact of growing-season warming on spring or autumn phenological events under continued climate warming. It is, therefore, crucial to examine the temporal variability in the response of tree phenology to growing-season warming to accurately forecast future changes in tree phenology and carbon cycling.

In this study, we combined long-term and large-scale ground phenological observations and remote-sensing datasets across the deciduous broadleaved forests in the Northern Hemisphere to examine and compare the temporal changes in the effects of growing-season warming on spring and autumn phenology. To clarify the physiological mechanisms under warming-induced changes in tree phenology, we further examined the photosynthetic productivity in response to growing-season warming. We hypothesized that the advancement of tree seasonal activities is decelerating when the temperature exceeds the optimum for photosynthesis under continued warming scenarios.

RESULTS

To examine the warming effects on tree phenology, we first collected around 700,000 ground observations of 23 temperate tree species between 1983 and 2014 from the Pan European Phenology (PEP725) network. There were 417,777 records of leaf unfolding and 271,928 records of leaf senescence selected from 20 species and 13 species, respectively (Table S1). The dates of leaf unfolding and leaf senescence were used to represent the start (SOS) and the end (EOS) of growing season. Because *Aesculus hippocastanum* (*A. hippocastanum*), *Betula pendula* (*B. pendula*), *Fagus sylvatica* (*F. sylvatica*), and *Quercus robur* (*Q. robur*) accounted for a majority of the total observations of all the 23 species and had both spring and autumn phenology records, we mainly showed the results based on these four representative species, and other species were used to further ensure the robustness and generality of our results. Using the PEP725 network, we calculated the temperature sensitivity (S_T) of SOS and EOS ($S_{T\text{-}SOS}$/$S_{T\text{-}EOS}$, advanced days per degree Celsius) between 1983 and 2014 for each species at each site in the PEP725 dataset. The $S_{T\text{-}SOS}$ and $S_{T\text{-}EOS}$ between 1983 and 2014 based on the complementary phenological metrics extracted from the Global Inventory Monitoring and Modeling System (GIMMS) Normalized Difference Vegetation Index-3rd generation ($NDVI_{3g}$) dataset were calculated as well. Using gross primary productivity (GPP) data modeled from the revised eddy covariance-light use efficiency (EC-LUE) model (GPP_{GLASS}) between 1983 and 2014, we further calculated the S_T of GPP ($S_{T\text{-}GPP}$, increased gC $m^{-2}d^{-1}$ per degree Celsius) to analyze the response of photosynthetic carbon uptake to growing-season warming. Considering the tree species selected from the PEP725 dataset were deciduous broadleaved tree species, we focused on the pixels of deciduous broadleaved forests in remote-sensing data across the Northern Hemisphere.

The $S_{T\text{-}SOS}$ was calculated as the slope of linear regression of the SOS against the T_{GS} of the previous year. The $S_{T\text{-}EOS}$ and $S_{T\text{-}GPP}$ were calculated as the slopes of linear regression of EOS or GPP in response to the T_{GS} of the current year. Positive and negative $S_{T\text{-}SOS}$ and $S_{T\text{-}EOS}$ indicated advanced and delayed days per degree Celsius respectively, and positive $S_{T\text{-}GPP}$ indicated increased carbon assimilation per degree Celsius. To assess temporal changes in the warming effects on tree phenology and productivity, we calculated the S_T (i.e., $S_{T\text{-}SOS}$, $S_{T\text{-}EOS}$, and $S_{T\text{-}GPP}$) based on a 15-year moving window, and compared the difference in the S_T (i.e., $S_{T\text{-}SOS}$, $S_{T\text{-}EOS}$, and $S_{T\text{-}GPP}$) between the coldest (1984–1998) and warmest (1999–2013) periods. In addition, we calculated the mean T_{GS} and vapor pressure deficit (VPD) based on the same window and examined the changes in $S_{T\text{-}SOS}$, $S_{T\text{-}EOS}$, and $S_{T\text{-}GPP}$ in response to rising temperature and VPD using linear regressions. To explore the relationship between photosynthetic carbon uptake and tree phenology, we further examined the correlation relationships between $S_{T\text{-}GPP}$ and S_T of tree phenology (i.e., $S_{T\text{-}SOS}$ and $S_{T\text{-}EOS}$). We also compared the overall effects of growing-season warming on spring and autumn phenology, by calculating $S_{T\text{-}SOS}$ and $S_{T\text{-}EOS}$ throughout the study periods from 1983 to 2014. One-way analysis of variance (ANOVA) was used to compare the difference between $S_{T\text{-}SOS}$ and $S_{T\text{-}EOS}$ based on the PEP725 and GIMMS $NDVI_{3g}$ datasets, separately.

Temporal change in growing-season warming effect on spring phenology

Here, we found $S_{T\text{-}SOS}$ based on previous T_{GS} showed a significant decline across all the four widely distributed temperate deciduous tree species in the PEP725 dataset (Figure 1A). The $S_{T\text{-}SOS}$ was significantly higher during the cold period (1984–1998) than during the warm period (1999–2013) across all the four representative species (Figure 1A). To test the generality of the results, we further examined and compared the warming effects on SOS in cold and warm periods by pooling the SOS records of all the 20 species selected in the PEP725 dataset using a linear mixed model (Table S2). The response variable was the SOS, and T_{GS}, the period (a categorical variable with two levels, cold and warm), and their interaction term were the predictor variables with random intercepts among sites and species. It was shown that the advancing response of SOS to increasing T_{GS} was also significantly lower during the warm than the cold period (Table S2). In addition, we observed a significant decrease in $S_{T\text{-}SOS}$ across all four representative species with the rising T_{GS} between 1983 and 2014 (Figure 1B).

Using the GIMMS $NDVI_{3g}$ dataset, we also observed a declining trend in $S_{T\text{-}SOS}$ across the northern deciduous broadleaved forests, and the $S_{T\text{-}SOS}$ was significantly higher during the cold than that during the warm period (Figure 1C).

Please cite this article in press as: Qiao et al., Accelerating effects of growing-season warming on tree seasonal activities are progressively disappearing, Current Biology (2023), https://doi.org/10.1016/j.cub.2023.07.030

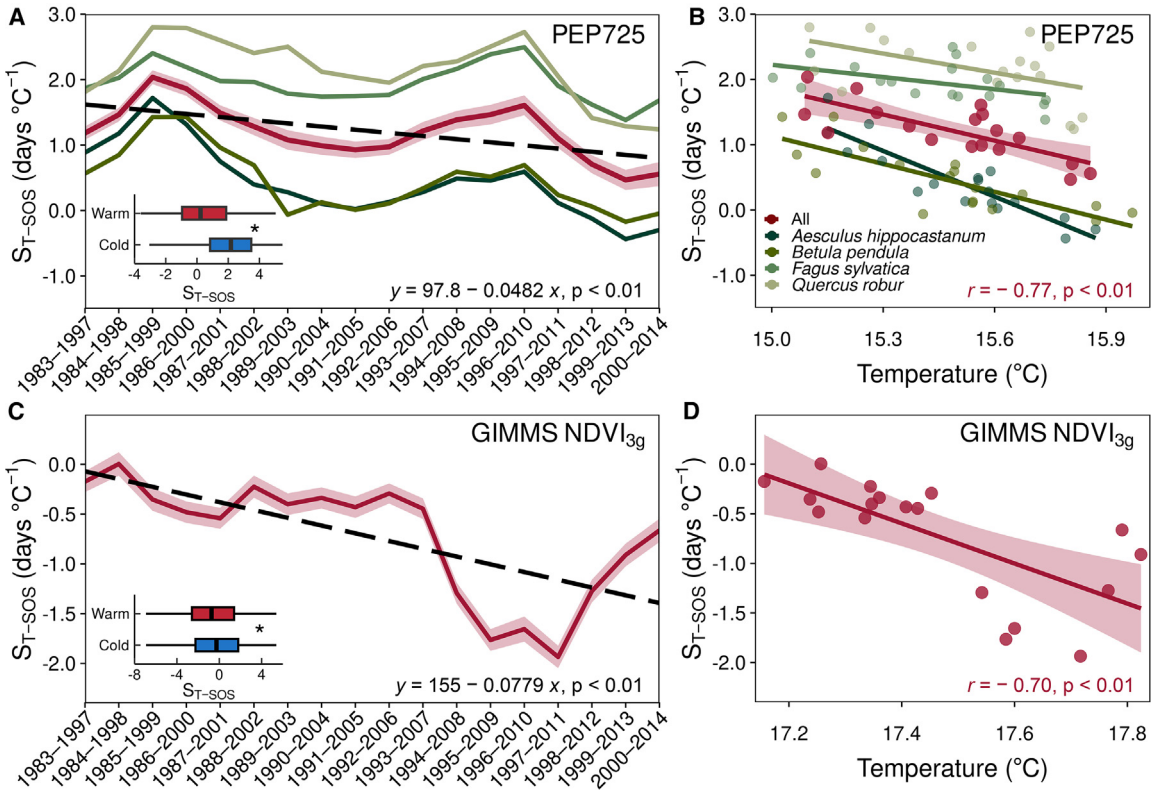

Figure 1. Changes in temperature sensitivities of spring phenology (S_{T-SOS}, advanced days per degree Celsius) from 1983 to 2014 using a 15-year sliding window and in response to the increasing temperature during the previous growing season

The S_{T-SOS} were calculated based on SOS of the four deciduous tree species in the PEP725 dataset (A and B) and that of deciduous broadleaved forest in the GIMMS NDVI$_{3g}$ phenological product (C and D). The red lines in (A) and (B) denote the mean S_{T-SOS} across all the four species, while those in (C) and (D) denote the mean across all pixels. The light red areas indicate the 95% confidence intervals. The black dashed line indicates the significant linear changing trend ($p < 0.01$) of S_{T-SOS} across species, and the regression equation was presented. The r indicates the linear correlation. The inset plots in (A) and (C) showed the S_{T-SOS} during the coldest (1984–1998) and the warmest (1999–2013) 15-year periods in 1983–2014, where the length of the box denotes the interquartile range, and its center black line denotes the median. Values beyond the whiskers were hidden. One-way analysis of variance (ANOVA) was used to test the statistically significant differences (*$p < 0.01$).

See also Figures S1, S3, and S5 and Tables S1 and S2.

Additionally, the S_{T-SOS} significantly decreased with rising T_{GS} in deciduous broadleaved forests (Figure 1D). Mean S_{T-SOS} based on PEP725 dataset was significantly higher than that based on the GIMMS NDVI$_{3g}$ dataset (Figure S1A), while mean T_{GS} across all the sites in the PEP725 dataset was significantly lower than that of all the pixels of deciduous broadleaved forests in the GIMMS NDVI$_{3g}$ dataset (Figure S1B). This also suggested that the S_{T-SOS} showed a significant decline with the increase in T_{GS}.

Temporal change in growing-season warming effect on autumn phenology

As with the S_{T-SOS}, the S_{T-EOS} based on the current T_{GS} showed a significant declining trend across all the four species in the PEP725 dataset (Figure 2A). The S_{T-EOS} gradually shifted from positive to negative from 1983 to 2014 (Figure 2A), indicating a switch from the advancing to delaying effects of current growing-season warming on EOS. The S_{T-EOS} was significantly higher during the cold than that during the warm period across all the four representative species (Figure 2A). Results of the linear mixed model showed that the advancing response of EOS to increasing T_{GS} was significantly lower during the warm than the cold period across all the 13 species selected in the PEP725 dataset (Table S2). Additionally, we observed a significant negative correlation between S_{T-EOS} and rising T_{GS} across all four representative species (Figure 2B). Using the remote-sensing data, a similar declining trend, with S_{T-EOS} from positive to negative, was also observed across the deciduous broadleaved forests in the Northern Hemisphere. The remote-sensing-based S_{T-EOS} was significantly higher during the cold than that during the warm period (Figure 2C). Consistently, the S_{T-EOS} showed a significant decrease with rising T_{GS} in deciduous broadleaved forests (Figure 2D).

Temporal change in growing-season warming effect on productivity

Using the GPP$_{GLASS}$ dataset, we found S_{T-GPP} showed a declining trend over the past decades (Figure 3A). In addition, the S_{T-GPP} was significantly higher during the cold period than during the warm period (Figure 3A). We observed a significant negative correlation between S_{T-GPP} and mean T_{GS} across deciduous broadleaved forests (Figure 3B). Both S_{T-SOS} and S_{T-EOS} showed a strong positive correlation with S_{T-GPP} (Figure 3C). We further

Please cite this article in press as: Qiao et al., Accelerating effects of growing-season warming on tree seasonal activities are progressively disappearing, Current Biology (2023), https://doi.org/10.1016/j.cub.2023.07.030

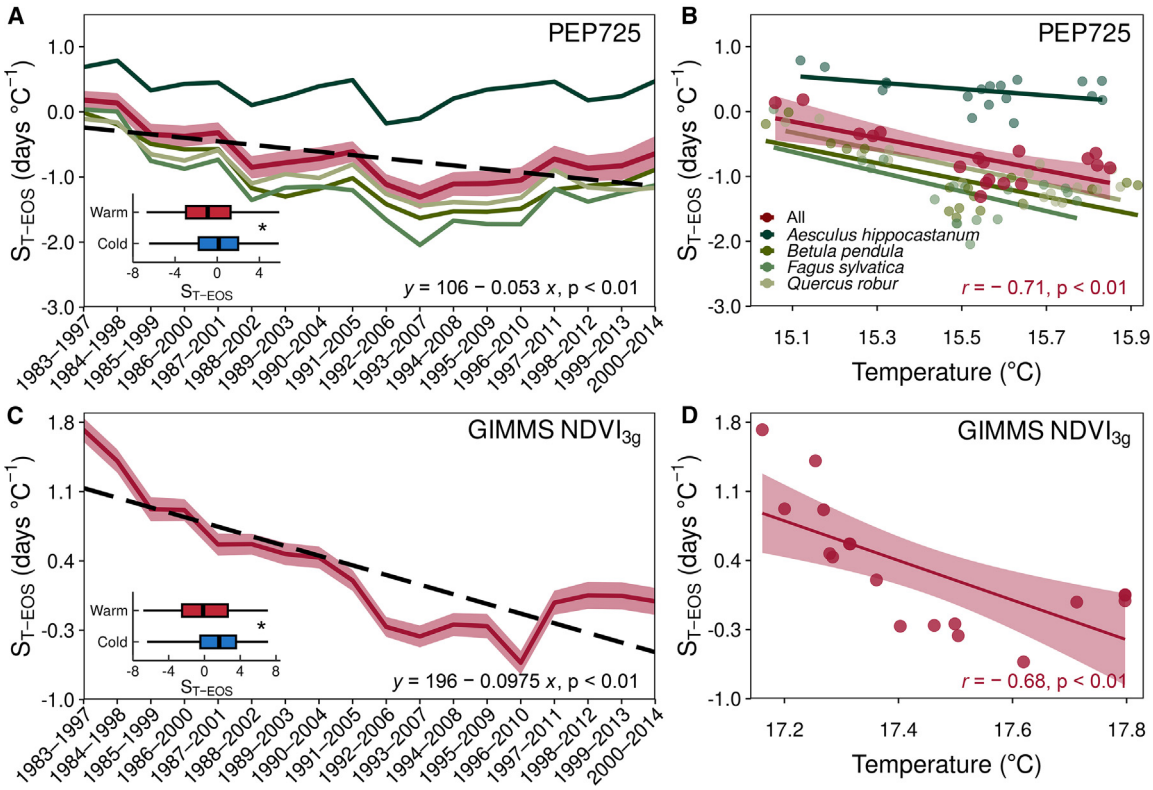

Figure 2. Changes in temperature sensitivities of autumn phenology (S_{T-EOS}, advanced days per degree Celsius) from 1983 to 2014 using a 15-year sliding window and in response to the increasing temperature during the current growing season

The S_{T-EOS} were calculated based on EOS of the four deciduous tree species in the PEP725 dataset (A and B) and that of deciduous broadleaved forest in the GIMMS $NDVI_{3g}$ phenological product (C and D). The red lines in (A) and (B) denote the mean S_{T-EOS} across all the four species, while those in (C) and (D) denote the mean across all pixels. The light red areas indicate the 95% confidence intervals. The black dashed line indicates the significant linear changing trend ($p < 0.01$) of S_{T-EOS} across species, and the regression equation was presented. The r indicates the linear correlation. The inset plots in (A) and (C) showed the S_{T-EOS} during the coldest (1984–1998) and the warmest (1999–2013) 15-year periods in 1983–2014, where the length of box denotes the interquartile range, and its center black line denotes the median. Values beyond the whiskers were hidden. One-way analysis of variance (ANOVA) was used to test the statistically significant differences (*$p < 0.01$).

See also Figures S4 and S5 and Tables S1 and S2.

observed that the S_{T-SOS} and S_{T-EOS} in PEP725 and GIMMS $NDVI_{3g}$, as well as the S_{T-GPP} based on GPP_{GLASS}, exhibited a significant decrease with the increasing VPD (Figure 4). We calculated the S_{T-GPP}, average T_{GS}, and VPD for each deciduous-broadleaved-forests site/pixel using the FLUXNET, global 'OCO-2' solar-induced chlorophyll fluorescence (GOSIF), and Global Land Surface Satellite (GLASS) GPP datasets and showed that the S_{T-GPP} underwent a consistently declining trend regardless of the GPP data sources, with the increased temperature and VPD during the growing season (Figure S2).

Comparison between spring and autumn phenology

The overall S_{T-SOS} throughout the study period during 1983–2014 was significantly higher than S_{T-EOS}, using both PEP725 and GIMMS $NDVI_{3g}$ datasets (Figure 5). We observed significant differences between S_{T-SOS} and S_{T-EOS} for each species (Figure 5C). However, the S_{T-SOS} of *F. sylvatica* and *Q. robur* was significantly higher than that of *A. hippocastanum* and *B. pendula* (Table S3). By contrast, the S_{T-EOS} of *F. sylvatica*, *Q. robur*, and *B. pendula* was significantly lower than that of *A. hippocastanum* (Table S3).

DISCUSSION

Over the past decades, shifts in tree phenology due to climate warming have been widely reported based on temperature during the pre-season.[15,21] In fact, shifts in tree phenology are also linked to changes in growing-season photosynthetic carbon uptake.[9,11] However, current understanding of the temporal effects of growing-season warming on tree spring and autumn phenology is limited. Combining long-term and large-scale ground observations and remote-sensing data, we observed that warming temperatures during the growing season triggered earlier leaf-out and leaf senescence in temperate and boreal deciduous broadleaved forests. However, the accelerating effects of rising T_{GS} on both spring and autumn phenology are disappearing, with phenological events even shifting from advancing to delaying, under continued climate warming (Figure 6).

Trees assimilate and store carbohydrates during the growing season, which are used to protect cells from frost damage in winter and support bud or leaf growth in early spring.[22,23] Up to 95% of the non-structural carbohydrates (e.g., starch and

Please cite this article in press as: Qiao et al., Accelerating effects of growing-season warming on tree seasonal activities are progressively disappearing, Current Biology (2023), https://doi.org/10.1016/j.cub.2023.07.030

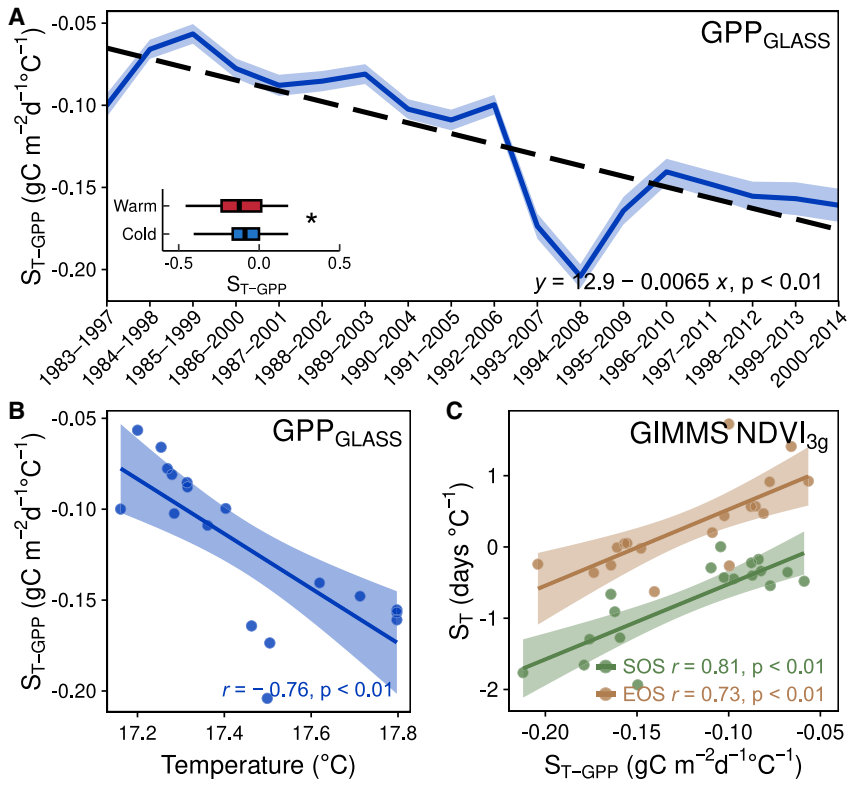

Figure 3. Changes in gross primary productivity (S_{T-GPP}, increased gC m^{-2}d^{-1} per degree Celsius) from 1983 to 2014 using a 15-year sliding window and the correlations between S_{T-GPP} and temperature sensitivities of spring or autumn phenology (S_{T-SOS}/S_{T-EOS}, advanced days per degree Celsius)

The decline trend of S_{T-GPP} in the deciduous broadleaved forest was showed in (A), and that in response to rising temperature during the current growing season was showed in (B). The correlations between S_{T-SOS} or S_{T-EOS} and S_{T-GPP} were showed in (C). The S_{T-GPP} was calculated based on GPP$_{GLASS}$. The S_{T-SOS} and S_{T-EOS} were calculated based on the GIMMS NDVI$_{3g}$ dataset. The blue line in (A) denotes the mean S_{T-GPP} across all pixels, while the black dashed line indicates the significant linear changing trend (p<0.01) of S_{T-GPP} across pixels, and the regression equation was presented. The shaded areas indicate the 95% confidence intervals. The *r* indicates the linear correlation. The inset plots in (A) showed the S_{T-GPP} during the coldest (1984–1998) and the warmest (1999–2013) 15-year periods in 1983–2014, where the length of box denotes the interquartile range, and its center black line denotes the median. Values beyond the whiskers were hidden. One-way analysis of variance (ANOVA) was used to test the statistically significant differences (* p < 0.01).
See also Figures S2, S5, and S6.

sugar) stored in the branches of *F. sylvatica* and *Quercus petraea* were used to support bud growth in the spring.[24] Phloem girdling experimental evidence showed that reduced carbon storage delayed spring leaf-out in temperate trees.[25] Therefore, a warmer growing season may drive earlier spring phenology in the successive year by increasing photosynthetic carbon assimilation and storage. However, canopy photosynthetic rates decrease when temperatures surpass the optimum.[26,27] Using remote-sensing-derived GPP data, here we observed a significant decline in the S_T of GPP over recent decades. Furthermore, the S_T of spring phenology showed a strong correlation with that of growing-season GPP. These findings suggested that the decline in S_{T-GPP} may partly explain the deceleration of advancing effects of previous growing-season warming on spring phenology. This provides new evidence that warming may influence spring phenology by altering the photosynthetic carbon uptake in the previous growing season in deciduous broadleaved trees in the Northern Hemisphere.

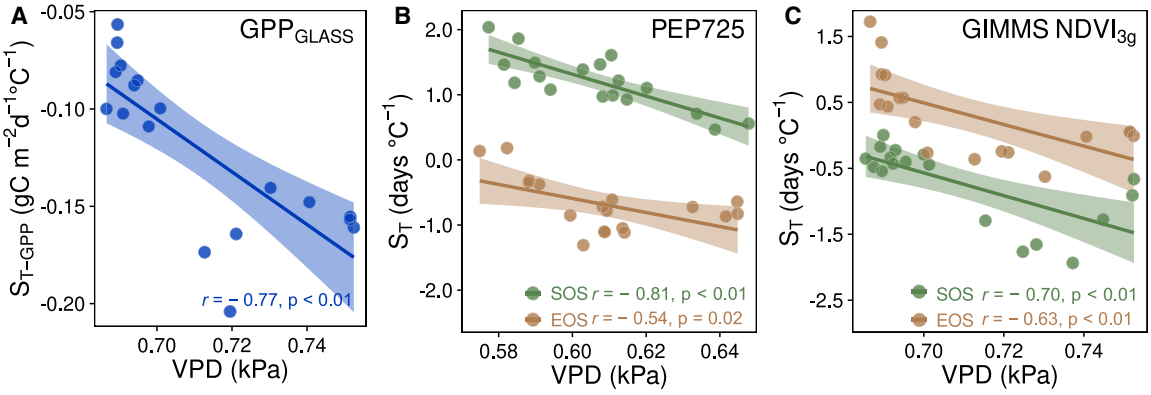

Figure 4. Linear relationships between vapor pressure deficit (VPD) and temperature sensitivities of gross primary productivity (S_{T-GPP}, increased gC m^{-2}d^{-1} per degree Celsius) and that of spring or autumn phenology (S_{T-SOS}/S_{T-EOS}, advanced days per degree Celsius)

In (A), the S_{T-GPP} was calculated based on GPP$_{GLASS}$. In (B) and (C), S_{T-SOS} and S_{T-EOS} were calculated based on the PEP725 dataset and the GIMMS NDVI$_{3g}$ dataset, respectively. Note that the mean S_{T-SOS}, S_{T-EOS}, and S_{T-GPP} were calculated using a 15-year sliding window. The shaded areas indicate the 95% confidence intervals. The linear correlations were presented.
See also Figures S2 and S4–S6.

Please cite this article in press as: Qiao et al., Accelerating effects of growing-season warming on tree seasonal activities are progressively disappearing, Current Biology (2023), https://doi.org/10.1016/j.cub.2023.07.030

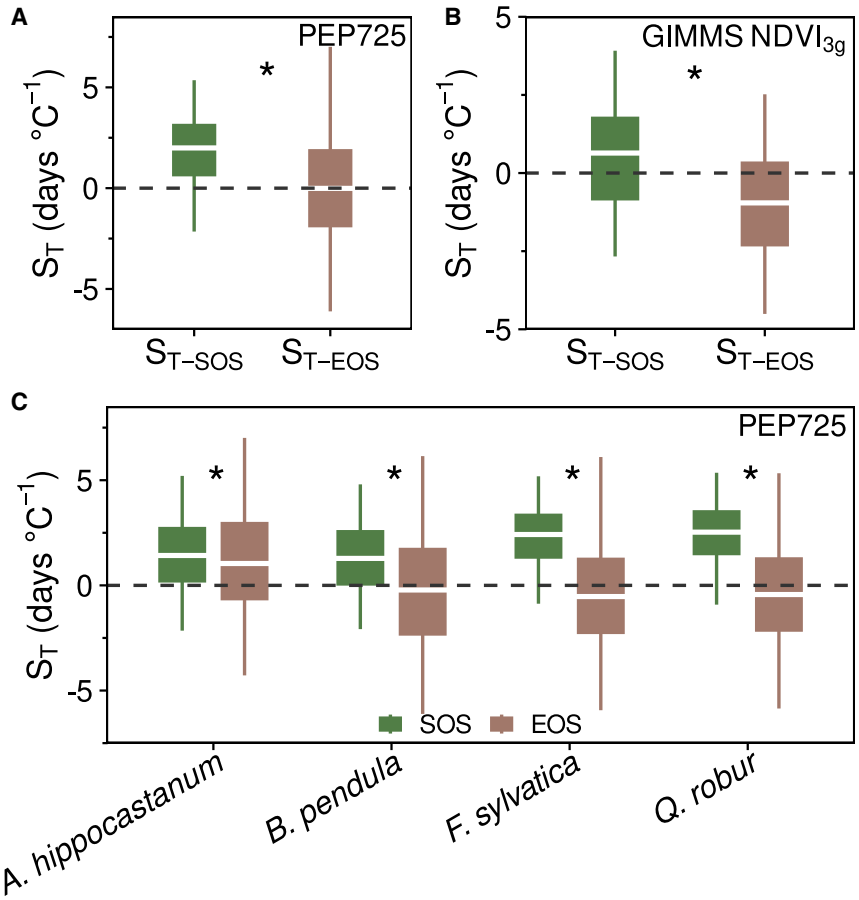

Figure 5. Differences between the temperature sensitivities of spring and autumn phenology ($S_{T\text{-}SOS}$ and $S_{T\text{-}EOS}$, advanced days per degree Celsius)

The $S_{T\text{-}SOS}$ and $S_{T\text{-}EOS}$ were calculated based on the PEP725 (A) and the GIMMS $NDVI_{3g}$ datasets (B) in 1983–2014, respectively. The $S_{T\text{-}SOS}$ and $S_{T\text{-}EOS}$ of the four deciduous species in the PEP725 dataset used in this study were further presented. The length of box denotes the interquartile range, and its center white line denotes the median. Values beyond the whiskers were hidden. The black dashed lines indicate S_T, which equals zero. One-way analysis of variance (ANOVA) was used to test the significance of the differences between the $S_{T\text{-}SOS}$ and $S_{T\text{-}EOS}$ (*$p < 0.01$).
See also Figure S5 and Tables S2 and S3.

Warming autumns can reduce the rate of chlorophyll degradation, enhance the activities of photosynthetic enzymes, and reduce the risk of late autumn frost,[28–30] ultimately delaying autumn phenology.[31,32] Meanwhile, the timing of leaf senescence is also linked to the maximum amount of assimilated carbon that can be stored in trees (or sink limitation of photosynthesis).[33] If warming (or other factors, e.g., elevated carbon dioxide and light levels) speeds up the rate of photosynthesis and the rate at which the maximum sugar storage capacity is reached, then leaf senescence may be advanced.[11] However, the reported relationships between autumn leaf senescence and photosynthetic carbon assimilation are contradictory. Combining ground observations and shade experiments, Zani et al. reported that a warmer growing season increased productivity and thus triggered earlier autumn leaf senescence in temperate deciduous trees.[11] Using observations from 40 eddy-covariance flux tower sites, Lu and Keenan found no significant negative relationship between growing-season photosynthesis and the timing of autumn leaf senescence since 2000.[12] According to $S_{T\text{-}EOS}$ calculated using the sliding window, we observed an advancement in autumn leaf senescence due to a warmer growing season before 2000. However, since 2000, the advancing effect of growing-season warming on leaf senescence progressively disappeared or even reversed, corresponding to a synchronized decrease in the warming effect on

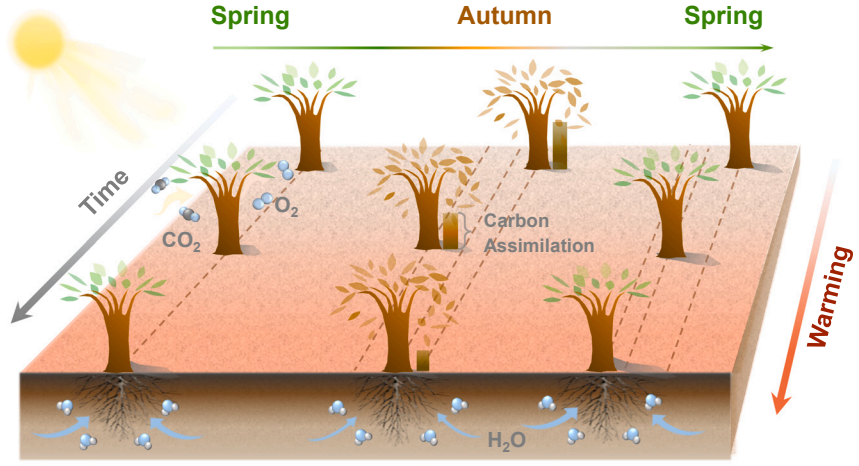

Figure 6. A diagram illustrating the temporal changes in the effects of growing-season warming on spring and autumn phenology of trees

The arrows indicate the growing-season warming over time. The three-column trees denote tree seasonal activities (phenological phenomena) in spring, autumn, and the next spring, respectively. The bars beside the trees indicate the rate of carbon assimilation during the growing season. The dashed lines signify the changes in the phenological timings as the growing-season warming continues over time (along the arrows). The growing-season warming induced the decline of trees' carbon assimilation. Warming during the growing season triggers earlier spring and autumn phenology in temperate and boreal deciduous broadleaved forests, but the acceleration of tree seasonal activities due to growing-season warming is progressively disappearing.

Please cite this article in press as: Qiao et al., Accelerating effects of growing-season warming on tree seasonal activities are progressively disappearing, Current Biology (2023), https://doi.org/10.1016/j.cub.2023.07.030

CellPress

photosynthetic productivity (Figure 3A). As a result, the nonlinear warming response of photosynthetic carbon assimilation demonstrated in our research reconciled, at least in part, the observed divergent responses of autumn senescence to growing-season warming and productivity.

The GPP simulation relies on accurate representations of multiple biophysical and biogeochemical processes that contributed significantly to the long-term vegetation production, such as CO_2 fertilization effect.[34] Here, we utilized the GLASS GPP, FLUXNET, and GOSIF GPP datasets to capture interannual GPP variation in response to climate change. Although uncertainty still exists in current GPP algorithms, irrespective of data sources, we consistently observed that $S_{T\text{-}GPP}$ exhibited a consistent decline as the temperature and VPD increased during the growing season. Under climate warming, rising temperature can commonly speed up photosynthetic rate within a certain range of temperature,[35] however, it may exponentially increase VPD, thus inducing stomatal closure and ultimately decreasing leaf photosynthetic rates.[20,36] Therefore, warming-induced water stress in trees may explain the observed decline in the $S_{T\text{-}GPP}$. To test this hypothesis, we further examined the relationship between $S_{T\text{-}GPP}$ and VPD and found that $S_{T\text{-}GPP}$ showed a significant decline with increased VPD, as did $S_{T\text{-}SOS}$ and $S_{T\text{-}EOS}$. These findings suggested that warming-induced water stress may explain the observed decline in the effects of growing-season warming on tree phenology by decreasing photosynthetic carbon uptake.

The phenological records from the PEP725 network are direct observations in the field, whereas phenological metrics extracted from the GIMMS $NDVI_{3g}$ dataset are based on an arbitrary inflection point assumption. In addition, the PEP725 dataset actually provides species-specific *in situ* phenology observations, whereas the satellite remote-sensing phenology product reflects the average phenological characteristics over the region scale. However, we consistently observed declining trends of $S_{T\text{-}SOS}$ and $S_{T\text{-}EOS}$ regardless of these inconsistencies. This reinforced the robustness of our findings and indicated the reliability when scaling up from high-quality field-collected phenology to coarse but larger-scale remote-sensing data.

Although a warmer growing season can influence both spring and autumn phenology by altering carbon uptake, spring phenology showed a significantly stronger response to T_{GS} than autumn phenology. In addition to temperature, photoperiod may influence phenological events in spring and autumn.[37,38] As the photoperiod remains unchanged across years for a given location, a relatively conservative climatic response is therefore expected when trees rely on the photoperiod to determine phenology.[38–40] Autumnal phenological events have been reported to be more sensitive to photoperiod compared with spring events.[38] For example, autumn leaf senescence often shows a more conservative warming response than spring leaf-out.[41] As such, seasonal-specific photoperiod sensitivity may explain why autumn phenology showed a weaker response to growing-season warming compared with spring phenology.[42] We further observed a significant difference in the warming responses of tree phenology among species. This could be also related to the species-specific difference in photoperiod sensitivity. It has been reported that *F. sylvatica* is more sensitive to photoperiod than *A. hippocastanum*,[43,44] which might account for why the observed warming response in *F. sylvatica* was lower than in *A. hippocastanum*.

STAR★METHODS

Detailed methods are provided in the online version of this paper and include the following:

- KEY RESOURCES TABLE
- RESOURCE AVAILABILITY
  - Lead contact
  - Materials availability
  - Data and code availability
- EXPERIMENTAL MODEL AND STUDY PARTICIPANT DETAILS
- METHOD DETAILS
  - Phenological data
  - Gross primary productivity data
  - Climate data
- QUANTIFICATION AND STATISTICAL ANALYSIS
  - Growing-season warming effect on phenology
  - Growing-season warming effect on productivity

SUPPLEMENTAL INFORMATION

Supplemental information can be found online at https://doi.org/10.1016/j.cub.2023.07.030.

ACKNOWLEDGMENTS

We acknowledge all members of the PEP725 network for collecting and providing the phenological data. This research was funded by the National Natural Science Foundation of China (32271833). N.G.S. acknowledges support from Texas Tech University.

AUTHOR CONTRIBUTIONS

L.C. designed the research. Y.Q. and H.G. performed the data analysis. L.C. and Y.Q. wrote the paper with the inputs of H.X., Q.M., X.Z., Q.Y., J.G., Y.Y., S.R., N.G.S., and J.L. All authors contributed to the interpretation of the results and approved the final manuscript.

DECLARATION OF INTERESTS

The authors declare no competing interests.

INCLUSION AND DIVERSITY

We support inclusive, diverse, and equitable conduct of research.

Received: April 16, 2023
Revised: June 19, 2023
Accepted: July 19, 2023
Published: August 10, 2023

REFERENCES

1. Montgomery, R.A., Rice, K.E., Stefanski, A., Rich, R.L., and Reich, P.B. (2020). Phenological responses of temperate and boreal trees to warming depend on ambient spring temperatures, leaf habit, and geographic range. Proc. Natl. Acad. Sci. USA *117*, 10397–10405. https://doi.org/10.1073/pnas.1917508117.
2. Richardson, A.D., Keenan, T.F., Migliavacca, M., Ryu, Y., Sonnentag, O., and Toomey, M. (2013). Climate change, phenology, and phenological

Please cite this article in press as: Qiao et al., Accelerating effects of growing-season warming on tree seasonal activities are progressively disappearing, Current Biology (2023), https://doi.org/10.1016/j.cub.2023.07.030

control of vegetation feedbacks to the climate system. Agric. For. Meteorol. *169*, 156–173. https://doi.org/10.1016/j.agrformet.2012.09.012.

3. Piao, S., Tan, J., Chen, A., Fu, Y.H., Ciais, P., Liu, Q., Janssens, I.A., Vicca, S., Zeng, Z., Jeong, S.J., et al. (2015). Leaf onset in the northern hemisphere triggered by daytime temperature. Nat. Commun. *6*, 6911. https://doi.org/10.1038/ncomms7911.
4. Beil, I., Kreyling, J., Meyer, C., Lemcke, N., and Malyshev, A.V. (2021). Late to bed, late to rise—warmer autumn temperatures delay spring phenology by delaying dormancy. Glob. Change Biol. *27*, 5806–5817. https://doi.org/10.1111/gcb.15858.
5. Asse, D., Chuine, I., Vitasse, Y., Yoccoz, N.G., Delpierre, N., Badeau, V., Delestrade, A., and Randin, C.F. (2018). Warmer winters reduce the advance of tree spring phenology induced by warmer springs in the Alps. Agric. For. Meteorol. *252*, 220–230. https://doi.org/10.1016/j.agrformet.2018.01.030.
6. Clark, J.S., Salk, C., Melillo, J., and Mohan, J. (2014). Tree phenology responses to winter chilling, spring warming, at north and south range limits. Funct. Ecol. *28*, 1344–1355. https://doi.org/10.1111/1365-2435.12309.
7. Li, M.H., Jiang, Y., Wang, A., Li, X., Zhu, W., Yan, C.F., Du, Z., Shi, Z., Lei, J., Schönbeck, L., et al. (2018). Active summer carbon storage for winter persistence in trees at the cold alpine treeline. Tree Physiol. *38*, 1345–1355. https://doi.org/10.1093/treephys/tpy020.
8. Richardson, A.D., Hollinger, D.Y., Dail, D.B., Lee, J.T., Munger, J.W., and O'Keefe, J. (2009). Influence of spring phenology on seasonal and annual carbon balance in two contrasting New England forests. Tree Physiol. *29*, 321–331. https://doi.org/10.1093/treephys/tpn040.
9. Gu, H., Qiao, Y., Xi, Z., Rossi, S., Smith, N.G., Liu, J., and Chen, L. (2022). Warming-induced increase in carbon uptake is linked to earlier spring phenology in temperate and boreal forests. Nat. Commun. *13*, 3698. https://doi.org/10.1038/s41467-022-31496-w.
10. Piper, F.I., and Fajardo, A. (2023). Carbon stress causes earlier budbreak in shade-tolerant species and delays it in shade-intolerant species. Am. J. Bot. *110*, 1–11. https://doi.org/10.1002/ajb2.16129.
11. Zani, D., Crowther, T.W., Mo, L., Renner, S.S., and Zohner, C.M. (2020). Increased growing-season productivity drives earlier autumn leaf senescence in temperate trees. Science *370*, 1066–1071. https://doi.org/10.1126/science.abd8911.
12. Lu, X., and Keenan, T.F. (2022). No evidence for a negative effect of growing season photosynthesis on leaf senescence timing. Glob. Change Biol. *28*, 3083–3093. https://doi.org/10.1111/gcb.16104.
13. Huang, Y., Jiang, N., Shen, M., and Guo, L. (2020). Effect of preseason diurnal temperature range on the start of vegetation growing season in the Northern Hemisphere. Ecol. Indic. *112*, 106161. https://doi.org/10.1016/j.ecolind.2020.106161.
14. Vitasse, Y., Signarbieux, C., and Fu, Y.H. (2018). Global warming leads to more uniform spring phenology across elevations. Proc. Natl. Acad. Sci. USA *115*, 1004–1008. https://doi.org/10.1073/pnas.1717342115.
15. Fu, Y.H., Zhao, H., Piao, S., Peaucelle, M., Peng, S., Zhou, G., Ciais, P., Huang, M., Menzel, A., Peñuelas, J., et al. (2015). Declining global warming effects on the phenology of spring leaf unfolding. Nature *526*, 104–107. https://doi.org/10.1038/nature15402.
16. Yu, H., Luedeling, E., and Xu, J. (2010). Winter and spring warming result in delayed spring phenology on the Tibetan Plateau. Proc. Natl. Acad. Sci. USA *107*, 22151–22156. https://doi.org/10.1073/pnas.1012490107.
17. Wenden, B., Mariadassou, M., Chmielewski, F.M., and Vitasse, Y. (2020). Shifts in the temperature-sensitive periods for spring phenology in European beech and pedunculate oak clones across latitudes and over recent decades. Glob. Change Biol. *26*, 1808–1819. https://doi.org/10.1111/gcb.14918.
18. Grossiord, C., Buckley, T.N., Cernusak, L.A., Novick, K.A., Poulter, B., Siegwolf, R.T.W., Sperry, J.S., and McDowell, N.G. (2020). Plant responses to rising vapor pressure deficit. New Phytol. *226*, 1550–1566. https://doi.org/10.1111/nph.16485.
19. Yamori, W., Hikosaka, K., and Way, D.A. (2014). Temperature response of photosynthesis in C_3, C_4, and CAM plants: temperature acclimation and temperature adaptation. Photosynth. Res. *119*, 101–117. https://doi.org/10.1007/s11120-013-9874-6.
20. Lin, Y.S., Medlyn, B.E., and Ellsworth, D.S. (2012). Temperature responses of leaf net photosynthesis: the role of component processes. Tree Physiol. *32*, 219–231. https://doi.org/10.1093/treephys/tpr141.
21. Güsewell, S., Furrer, R., Gehrig, R., and Pietragalla, B. (2017). Changes in temperature sensitivity of spring phenology with recent climate warming in Switzerland are related to shifts of the preseason. Glob. Change Biol. *23*, 5189–5202. https://doi.org/10.1111/gcb.13781.
22. Kaurin, A., Junttila, O., and Hanson, J. (1981). Seasonal changes in frost hardiness in cloudberry (*Rubus chamaemorus*) in relation to carbohydrate content with special reference to sucrose. Physiol. Plant. *52*, 310–314. https://doi.org/10.1111/j.1399-3054.1981.tb08512.x.
23. Shahba, M.A., Qian, Y.L., Hughes, H.G., Koski, A.J., and Christensen, D. (2003). Relationships of soluble carbohydrates and freeze tolerance in saltgrass. Crop Sci. *43*, 2148–2153. https://doi.org/10.2135/cropsci2003.2148.
24. Klein, T., Vitasse, Y., and Hoch, G. (2016). Coordination between growth, phenology and carbon storage in three coexisting deciduous tree species in a temperate forest. Tree Physiol. *36*, 847–855. https://doi.org/10.1093/treephys/tpw030.
25. Amico Roxas, A.A., Orozco, J., Guzmán-Delgado, P., and Zwieniecki, M.A. (2021). Spring phenology is affected by fall non-structural carbohydrate concentration and winter sugar redistribution in three Mediterranean nut tree species. Tree Physiol. *41*, 1425–1438. https://doi.org/10.1093/treephys/tpab014.
26. Huang, M., Piao, S., Ciais, P., Peñuelas, J., Wang, X., Keenan, T.F., Peng, S., Berry, J.A., Wang, K., Mao, J., et al. (2019). Air temperature optima of vegetation productivity across global biomes. Nat. Ecol. Evol. *3*, 772–779. https://doi.org/10.1038/s41559-019-0838-x.
27. Duffy, K.A., Schwalm, C.R., Arcus, V.L., Koch, G.W., Liang, L.L., and Schipper, L.A. (2021). How close are we to the temperature tipping point of the terrestrial biosphere? Sci. Adv. *7*, eaay1052. https://doi.org/10.1126/sciadv.aay1052.
28. Fracheboud, Y., Luquez, V., Björkén, L., Sjödin, A., Tuominen, H., and Jansson, S. (2009). The control of autumn senescence in European aspen. Plant Physiol. *149*, 1982–1991. https://doi.org/10.1104/pp.108.133249.
29. Shi, C., Sun, G., Zhang, H., Xiao, B., Ze, B., Zhang, N., and Wu, N. (2014). Effects of warming on chlorophyll degradation and carbohydrate accumulation of alpine herbaceous species during plant senescence on the Tibetan Plateau. PLoS One *9*, e107874. https://doi.org/10.1371/journal.pone.0107874.
30. Yang, Y., Guan, H., Shen, M., Liang, W., and Jiang, L. (2015). Changes in autumn vegetation dormancy onset date and the climate controls across temperate ecosystems in China from 1982 to 2010. Glob. Change Biol. *21*, 652–665. https://doi.org/10.1111/gcb.12778.
31. Delpierre, N., Dufrêne, E., Soudani, K., Ulrich, E., Cecchini, S., Boé, J., and François, C. (2009). Modelling interannual and spatial variability of leaf senescence for three deciduous tree species in France. Agric. For. Meteorol. *149*, 938–948.
32. Liu, Q., Fu, Y.H., Zhu, Z., Liu, Y., Liu, Z., Huang, M., Janssens, I.A., and Piao, S. (2016). Delayed autumn phenology in the Northern Hemisphere is related to change in both climate and spring phenology. Glob. Change Biol. *22*, 3702–3711. https://doi.org/10.1111/gcb.13311.
33. Li, L., Wang, X., and Manning, W.J. (2019). Effects of elevated CO_2 on leaf senescence, leaf nitrogen resorption, and late-season photosynthesis in *Tilia americana* L. Front. Plant Sci. *10*, 1217. https://doi.org/10.3389/fpls.2019.01217.
34. Kolby Smith, W., Reed, S.C., Cleveland, C.C., Ballantyne, A.P., Anderegg, W.R.L., Wieder, W.R., Liu, Y.Y., and Running, S.W. (2016). Large divergence of satellite and Earth system model estimates of global terrestrial CO_2 fertilization. Nat. Clim. Change *6*, 306–310. https://doi.org/10.1038/nclimate2879.

Please cite this article in press as: Qiao et al., Accelerating effects of growing-season warming on tree seasonal activities are progressively disappearing, Current Biology (2023), https://doi.org/10.1016/j.cub.2023.07.030

35. Berry, J., and Bjorkman, O. (1980). Photosynthetic response and adaptation to temperature in higher plants. Annu. Rev. Plant Physiol. *31*, 491–543. https://doi.org/10.1146/annurev.pp.31.060180.002423.

36. McDowell, N.G. (2011). Mechanisms linking drought, hydraulics, carbon metabolism, and vegetation mortality. Plant Physiol. *155*, 1051–1059. https://doi.org/10.1104/pp.110.170704.

37. Körner, C., and Basler, D. (2010). Phenology under global warming. Science *327*, 1461–1462. https://doi.org/10.1126/science.1186473.

38. Way, D.A., and Montgomery, R.A. (2015). Photoperiod constraints on tree phenology, performance and migration in a warming world. Plant Cell Environ. *38*, 1725–1736. https://doi.org/10.1111/pce.12431.

39. Basler, D., and Körner, C. (2012). Photoperiod sensitivity of bud burst in 14 temperate forest tree species. Agric. For. Meteorol. *165*, 73–81. https://doi.org/10.1016/j.agrformet.2012.06.001.

40. Flynn, D.F.B., and Wolkovich, E.M. (2018). Temperature and photoperiod drive spring phenology across all species in a temperate forest community. New Phytol. *219*, 1353–1362. https://doi.org/10.1111/nph.15232.

41. Menzel, A., Sparks, T.H., Estrella, N., Koch, E., Aasa, A., Rein, A., Kerstin, A.-K., Peter, B., Ol'Ga, B., Agrita, B., et al. (2006). European phenological response to climate change matches the warming pattern. Glob. Change Biol. *12*, 1969–1976. https://doi.org/10.1111/j.1365-2486.2006.01193.x.

42. Gallinat, A., Primack, R., and Wagner, D. (2015). Autumn, the neglected season in climate change research. Trends Ecol. Evol. *30*, 169–176. https://doi.org/10.1016/j.tree.2015.03.016.

43. Chen, L., Huang, J.G., Ma, Q., Hänninen, H., Tremblay, F., and Bergeron, Y. (2019). Long-term changes in the impacts of global warming on leaf phenology of four temperate tree species. Glob. Change Biol. *25*, 997–1004. https://doi.org/10.1111/gcb.14496.

44. Vitasse, Y., and Basler, D. (2013). What role for photoperiod in the bud burst phenology of European beech. Eur. J. Forest Res. *132*, 1–8. https://doi.org/10.1007/s10342-012-0661-2.

45. Zheng, Y., Shen, R., Wang, Y., Li, X., Liu, S., Liang, S., Chen, J.M., Ju, W., Zhang, L., and Yuan, W. (2020). Improved estimate of global gross primary production for reproducing its long-term variation, 1982–2017. Earth Syst. Sci. Data *12*, 2725–2746. https://doi.org/10.5194/essd-12-2725-2020.

46. Li, X., and Xiao, J. (2019). Mapping photosynthesis solely from solar-induced chlorophyll fluorescence: a global, fine-resolution dataset of gross primary production derived from OCO-2. Remote Sens. *11*, 2563. https://doi.org/10.3390/rs11212563.

47. Templ, B., Koch, E., Bolmgren, K., Ungersböck, M., Paul, A., Scheifinger, H., Rutishauser, T., Busto, M., Chmielewski, F.M., Hájková, L., et al. (2018). Pan European Phenological database (PEP725): a single point of access for European data. Int. J. Biometeorol. *62*, 1109–1113. https://doi.org/10.1007/s00484-018-1512-8.

48. The National Center for Atmospheric Research (2018). Global GIMMS NDVI3g v1 dataset (1981–2015). A Big Earth Data Platform for Three Poles. http://poles.tpdc.ac.cn/en/data/9775f2b4-7370-4e5e-a537-3482c9a83d88/.

49. Pastorello, G., Trotta, C., Canfora, E., Chu, H., Christianson, D., Cheah, Y.W., Poindexter, C., Chen, J., Elbashandy, A., Humphrey, M., et al. (2020). The FLUXNET2015 dataset and the ONEFlux processing pipeline for eddy covariance data. Sci. Data *7*, 225. https://doi.org/10.1038/s41597-020-0534-3.

50. Abatzoglou, J.T., Dobrowski, S.Z., Parks, S.A., and Hegewisch, K.C. (2018). TerraClimate, a high-resolution global dataset of monthly climate and climatic water balance from 1958–2015. Sci. Data *5*, 170191. https://doi.org/10.1038/sdata.2017.191.

51. Friedl, M., and Sulla-Menashe, D. (2022). MODIS/Terra+Aqua Land Cover Type Yearly L3 Global 500 m SIN Grid V061. https://doi.org/10.5067/MODIS/MCD12Q1.061.

52. Leys, C., Ley, C., Klein, O., Bernard, P., and Licata, L. (2013). Detecting outliers: do not use standard deviation around the mean, use absolute deviation around the median. J. Exp. Soc. Psychol. *49*, 764–766. https://doi.org/10.1016/j.jesp.2013.03.013.

53. Wang, X., Xiao, J., Li, X., Cheng, G., Ma, M., Zhu, G., Altaf Arain, M., Andrew Black, T., and Jassal, R.S. (2019). No trends in spring and autumn phenology during the global warming hiatus. Nat. Commun. *10*, 2389. https://doi.org/10.1038/s41467-019-10235-8.

54. Zhang, X., Friedl, M.A., and Schaaf, C.B. (2009). Sensitivity of vegetation phenology detection to the temporal resolution of satellite data. Int. J. Remote Sens. *30*, 2061–2074. https://doi.org/10.1080/01431160802549237.

55. Loveland, T.R., and Belward, A.S. (1997). The International Geosphere Biosphere Programme Data and Information System global land cover data set (DISCover). Acta Astronaut. *41*, 681–689. https://doi.org/10.1016/S0094-5765(98)00050-2.

56. Liang, S., Cheng, J., Jia, K., Jiang, B., Liu, Q., Xiao, Z., Yao, Y., Yuan, W., Zhang, X., Zhao, X., et al. (2021). The Global Land Surface Satellite (GLASS) product suite. Bull. Am. Meteorol. Soc. *102*, E323–E337. https://doi.org/10.1175/BAMS-D-18-0341.1.

57. Yuan, W., Zheng, Y., Piao, S., Ciais, P., Lombardozzi, D., Wang, Y., Ryu, Y., Chen, G., Dong, W., Hu, Z., et al. (2019). Increased atmospheric vapor pressure deficit reduces global vegetation growth. Sci. Adv. *5*, eaax1396. https://doi.org/10.1126/sciadv.aax1396.

58. Hijmans, R.J. (2023). raster: geographic data analysis and modeling. https://CRAN.R-project.org/package=raster.

59. R Core Team (2020). R: a language and environment for statistical computing (R Foundation for Statistical Computing). https://www.R-project.org/.

60. Bradley, A.V., Gerard, F.F., Barbier, N., Weedon, G.P., Anderson, L.O., Huntingford, C., Aragão, L.E.O.C., Zelazowski, P., and Arai, E. (2011). Relationships between phenology, radiation and precipitation in the Amazon region. Glob. Change Biol. *17*, 2245–2260. https://doi.org/10.1111/j.1365-2486.2011.02405.x.

61. Wang, C., Cao, R., Chen, J., Rao, Y., and Tang, Y. (2015). Temperature sensitivity of spring vegetation phenology correlates to within-spring warming speed over the Northern Hemisphere. Ecol. Indic. *50*, 62–68. https://doi.org/10.1016/j.ecolind.2014.11.004.

62. Epskamp, S., and Fried, E.I. (2018). A tutorial on regularized partial correlation networks. Psychol. Methods *23*, 617–634. https://doi.org/10.1037/met0000167.

Please cite this article in press as: Qiao et al., Accelerating effects of growing-season warming on tree seasonal activities are progressively disappearing, Current Biology (2023), https://doi.org/10.1016/j.cub.2023.07.030

STAR★METHODS

KEY RESOURCES TABLE

REAGENT or RESOURCE	SOURCE	IDENTIFIER
Deposited data		
Analyzed code	This study	https://doi.org/10.5281/zenodo.8113301
Software and algorithms		
R version 4.1.2	R Core Team	https://www.r-project.org/
Other		
PEP725 phenology dataset	PEP725 network	http://www.pep725.eu/
GIMMS $NDVI_{3g}$ dataset	CASEarth	http://poles.tpdc.ac.cn/en/data/9775f2b4-7370-4e5e-a537-3482c9a83d88/
International Geosphere-Biosphere Programme (IGBP) classification	EARTHDATA	https://lpdaac.usgs.gov/products/mcd12q1v061/
GLASS GPP dataset	Zheng et al.[45]	https://doi.org/10.6084/m9.figshare.8942336.v3
FLUXNET GPP dataset	FLUXNET network	https://fluxnet.org/data/fluxnet2015-dataset/
GOSIF GPP dataset	Li and Xiao[46]	https://globalecology.unh.edu/data/GOSIF-GPP.html
TerraClimate dataset	Climatology Lab	https://www.climatologylab.org/terraclimate.html

RESOURCE AVAILABILITY

Lead contact

Further information and requests for resources and reagents should be directed to and will be fulfilled by the lead contact, Lei Chen (lei.chen1029@gmail.com).

Materials availability

This study did not generate new unique reagents.

Data and code availability

The phenology, gross primary productivity, climate and land cover datasets are publicly available. DOIs are listed in the key resources table.

All original code has been deposited at Zenodo and is publicly available as of the date of publication. The DOI is listed in the key resources table.

Any additional information required to reanalyze the data reported in this paper is available from the lead contact upon request.

EXPERIMENTAL MODEL AND STUDY PARTICIPANT DETAILS

The phenological datasets of PEP725 and GIMMS $NDVI_{3g}$ were downloaded from PEP725 network[47] and CASEarth,[48] respectively. The gross primary productivity datasets of GLASS, FLUXNET and GOSIF were downloaded from Zheng et al.,[45] FLUXNET network[49] and Li and Xiao,[46] respectively. The climate dataset affiliated to TerraClimate was downloaded from Climatology Lab.[50] The MODIS Global 500 m Terra and Aqua combined the yearly gridded land cover product (MCD12Q1 IGBP) was from EARTHDATA.[51]

METHOD DETAILS

Phenological data

PEP725 network

Ground observation phenological data was obtained from the Pan European Phenology (PEP725) network (http://www.pep725.eu/),[47] which is one of the largest phenology databases worldwide and provides open-access *in situ* observations. Here, the phenological stages were defined according to the BBCH code (Biologische Bundesanstalt, Bundessortenamt and Chemische Industrie), and the dates of the phenological stages were expressed as the day of the year (DOY). We selected leaf unfolding (BBCH 11, the date when first leaf stalk was visible) and leaf senescence (BBCH 94, the date when autumn leaves colored half percent of the whole tree) dates in the PEP725 dataset to represent spring and autumn phenology, representing the start (SOS) and the end (EOS) of season,

Please cite this article in press as: Qiao et al., Accelerating effects of growing-season warming on tree seasonal activities are progressively disappearing, Current Biology (2023), https://doi.org/10.1016/j.cub.2023.07.030

respectively. Records of leaf unfolding or leaf senescence dates exceeding 2.5 times the median absolute deviation (MAD) were considered as outliers and removed,[52] and sites with at least five years of observations were excluded. We preliminarily selected 417,777 spring phenological records of 20 temperate tree species at 3,554 sites and 271,928 autumn phenological records of 13 temperate tree species at 3,510 sites between 1983 and 2014 (Table S1). Among the 23 unduplicated species available (a total of 3,185 unduplicated sites), *Aesculus hippocastanum* (*A. hippocastanum*), *Betula pendula* (*B. pendula*), *Fagus sylvatica* (*F. sylvatica*), and *Quercus robur* (*Q. robur*) had not only both spring and autumn phenology records but 435,689 phenological records accounting for more than 55% of the total observations. Thus, we mainly presented the results based on the four representative species. The other species were used to test the robustness and generality of the results obtained from the abovementioned four species (Table S2).

GIMMS NDVI$_{3g}$ dataset

In addition to the ground-based phenological data in Europe, we downloaded the third-generation Normalized Difference Vegetation Index-3rd generation (NDVI$_{3g}$) of NOAA Global Inventory Monitoring and Modeling System (GIMMS) between 1983 and 2014 with a spatial resolution of 0.083° (~8 km) from http://poles.tpdc.ac.cn/en/data/9775f2b4-7370-4e5e-a537-3482c9a83d88/. We selected areas outside the tropics with clear seasonal phenological cycles. Pixels with annual mean NDVI < 0.1 were considered as non-vegetated areas and excluded from the successive analyses. The Savizky-Golay smooth method was applied to minimize the noise before extracting SOS and EOS.[53] The SOS and EOS were derived by the double logistic function, an inflection point detection method.[54] The SOS after the end of June and the EOS before that date were considered as outliers. We focused on remote-sensing-based phenological metrics in deciduous broadleaved forests in the Northern Hemisphere to ensure the comparability among phenological datasets, as all the selected tree species from the PEP725 dataset were deciduous broadleaved. The annual International Geosphere-Biosphere Programme (IGBP) classification[55] from MODIS Land Cover Type Product (MCD12Q1)[51] was used to classify the vegetation type in remote sensing datasets.

Gross primary productivity data

We obtained monthly GPP data from Global Land Surface Satellite (GLASS) product with a spatial resolution of 0.05° from 1983 to 2014.[45,56] This dataset is simulated based on the revised Eddy Covariance–Light Use Efficiency (EC-LUE) model, which integrates the impacts of several environmental variables, such as atmospheric CO_2 concentrations, radiation fluxes, and VPD.[57] As with the phenological data, we focused on GPP_{GLASS} data across deciduous broadleaved forests in the Northern Hemisphere based on the annual IGBP classification.

The daily GPP data from FLUXNET[49] and global 'OCO-2' solar-induced chlorophyll fluorescence (GOSIF)[46] datasets were also used to further validate the reliability of our results. We used FLUXNET-GPP variable (GPP_NT_VUT_REF) estimated by the nighttime partitioning method, which was improved for reproducing the long-term variation of global gross primary production. The GOSIF dataset provides SIF-derived GPP data with a fine spatial and temporal resolution (0.05° and 8-day, respectively) from 2000 to 2020. We also focused on FLUXNET and GOSIF datasets across deciduous broadleaved forests in the Northern Hemisphere based on the IGBP classification.

Climate data

Gridded daily mean temperature, minimum temperature, solar radiation, precipitation and vapor pressure deficit (VPD) were derived from TerraClimate,[50] a long time-scale climate dataset with a spatial resolution of ~4 km. We applied a bilinear interpolation method in "raster" package[58] to extract the monthly climate data of the phenological sites in R version 4.1.2.[59] In order to ensure consistency and reduce uncertainty of data analyses, we resampled GIMMS NDVI$_{3g}$, GPP_{GLASS} and GPP_{SIF} datasets to a spatial resolution of 4 km as with TerraClimate dataset.[50]

QUANTIFICATION AND STATISTICAL ANALYSIS

Growing-season warming effect on phenology

We calculated the temperature sensitivity (S_T) of leaf phenology ($S_{T\text{-}SOS}$/$S_{T\text{-}EOS}$, advanced days per degree Celsius). The $S_{T\text{-}SOS}$ was calculated as the slope of linear regressions of the SOS against the growing-season temperature (T_{GS}) of the previous year, while the $S_{T\text{-}EOS}$ was calculated as the slopes of linear regressions of EOS in response to the T_{GS} of the current year. Mean dates of SOS and EOS were DOY 116 and DOY 288 respectively across the deciduous broadleaved forests in the Northern Hemisphere, where the period between May and September was considered as the growing season. $S_{T\text{-}SOS}$ and $S_{T\text{-}EOS}$ were calculated for each species per site using the PEP725 dataset, or calculated per pixel using phenological data derived from the GIMMS NDVI$_{3g}$ dataset.

In addition to temperature, other climate factors, especially solar radiation and precipitation, may also influence tree phenology by altering growing-season leaf photosynthesis.[60] Spring and autumn temperatures also act as the driver of spring and autumn phenology, respectively.[11,61] To ensure the robustness of results, partial correlation analysis was used to exclude confounding effects,[62] we first excluded potential co-variate effects of solar radiation and precipitation of growing season and spring temperature (averaged mean temperature of the two months before dates of SOS) or autumn temperature (averaged minimum temperature of the two months before dates of EOS). After filtering the outliers based on the 95% confidence intervals of the absolute partial correlation coefficients, we calculated the S_T of tree phenology of all four representative species between 1983 and 2014 using a 15-year moving window to examine the temporal change in the warming effect on tree phenology. To evaluate the influence of the size of moving windows, we also applied 10- and 20-year moving windows, and found similar trends (Figures S3 and S4). Linear regression was

Please cite this article in press as: Qiao et al., Accelerating effects of growing-season warming on tree seasonal activities are progressively disappearing, Current Biology (2023), https://doi.org/10.1016/j.cub.2023.07.030

used to examine the temporal trends in the mean S_T of spring and autumn phenology. And we further compared the difference in the S_T of tree phenology between the coldest (1984−1998) and warmest (1999−2013) periods using one-way analysis of variance (ANOVA). Here the coldest and warmest periods were defined based on the average T_{GS} calculated by a 15-year moving window (Figure S5). Furthermore, we calculated the mean T_{GS} and VPD in each 15-year sliding window and examined the changes in the S_T of tree phenology ($S_{T\text{-}SOS}$ and $S_{T\text{-}EOS}$) in response to rising temperature and VPD using linear regression.

To test the generality of the results, we enlarged our species using PEP725 data (all the selected 20 and 13 species for SOS and EOS, respectively) to compare the overall effects of T_{GS} on tree phenology in the coldest and warmest periods using linear mixed models. In the models, the response variable was the SOS or EOS, while the T_{GS} and interaction term between T_{GS} and the period (factor variable with two levels: cold and warm) were set as the explanatory variables, with random intercepts among sites and species. One-way analysis of variance (ANOVA) was also used to examine the difference in the S_T of tree phenology ($S_{T\text{-}SOS}$ and $S_{T\text{-}EOS}$) between the PEP725 sites and GIMMS $NDVI_{3g}$ pixels as well as the average T_{GS} between the PEP725 sites and GIMMS $NDVI_{3g}$ pixels.

To examine and compare the overall effects of growing-season warming on spring and autumn phenology, we also calculate the $S_{T\text{-}SOS}$ and $S_{T\text{-}EOS}$ throughout the whole-time span (1983−2014 for PEP725 and GIMMS $NDVI_{3g}$). We then used one-way ANOVA and compared the difference between $S_{T\text{-}SOS}$ and $S_{T\text{-}EOS}$ based on the PEP725 and GIMMS $NDVI_{3g}$ datasets, separately. In addition, one-way ANOVA followed by Tukey's honestly significant difference (HSD) test were used to compare the difference in the $S_{T\text{-}SOS}$ and $S_{T\text{-}EOS}$ among tree species in the PEP725 dataset.

Growing-season warming effect on productivity

We calculated the temperature sensitivity (S_T) of GPP ($S_{T\text{-}GPP}$, increased gC $m^{-2}d^{-1}$ per degree Celsius), represented as the slope of linear regressions of the growing-season GPP (from May to September) against the T_{GS} of the current year. Before calculating the $S_{T\text{-}GPP}$, we excluded the potential effects of solar radiation and precipitation using a partial analysis between growing-season temperature and GPP, and filtered the outliers based on the 95% confidence intervals of the absolute partial correlation coefficients. We then calculated the $S_{T\text{-}GPP}$ at each pixel in the GPP_{GLASS} dataset using 10-, 15- and 20-year moving windows to examine the temporal changes in the warming effect on productivity, and still found similar trends (Figure S6). Consistent with S_T calculation of tree phenology, we selected the results based on the 15-year window to conduct the following analyses. Linear regression was used to examine the temporal trends in the mean $S_{T\text{-}GPP}$. Moreover, we compared the difference in the $S_{T\text{-}GPP}$ between the coldest (1984−1998) and warmest (1999−2013) periods. We examined the temporal trends of mean $S_{T\text{-}GPP}$ in response to rising temperatures and VPD under climate warming as well. To examine the effect of carbon assimilation on tree phenology, we matched the $S_{T\text{-}GPP}$ in the previous growing season with $S_{T\text{-}SOS}$, and that in the current growing season with $S_{T\text{-}EOS}$. We calculated the correlation coefficients between the S_T of tree phenology (i.e., $S_{T\text{-}SOS}$ and $S_{T\text{-}EOS}$) and the corresponding $S_{T\text{-}GPP}$.

Considering the limited length of time spans of the FLUXNET and GOSIF GPP datasets used in this study (1991−2014 and 2000−2014, respectively) compared with GLASS GPP data (from 1983 to 2014), notwithstanding their high accuracy, it is difficult to examine the temporal changes in the growing-season warming responses of GPP using moving windows (e.g., 10-, 15- and 20-year). Instead, we calculated the $S_{T\text{-}GPP}$ and examined the relationship between $S_{T\text{-}GPP}$ and average growing-season temperature and VPD for each site/pixel of deciduous broadleaved forests, using the FLUXNET, GOSIF and GLASS GPP datasets.

All the data analyses were conducted using R version 4.1.2.[59]